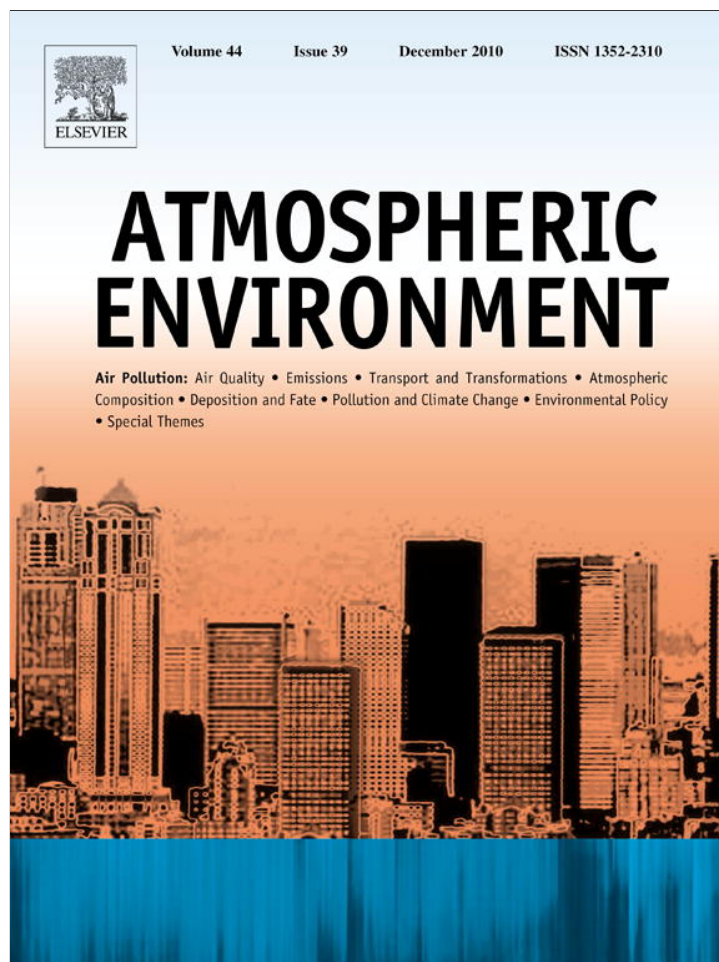


Provided for non-commercial research and education use.
Not for reproduction, distribution or commercial use.



This article appeared in a journal published by Elsevier. The attached copy is furnished to the author for internal non-commercial research and education use, including for instruction at the authors institution and sharing with colleagues.

Other uses, including reproduction and distribution, or selling or licensing copies, or posting to personal, institutional or third party websites are prohibited.

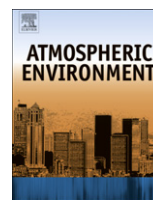
In most cases authors are permitted to post their version of the article (e.g. in Word or Tex form) to their personal website or institutional repository. Authors requiring further information regarding Elsevier's archiving and manuscript policies are encouraged to visit:

<http://www.elsevier.com/copyright>



Contents lists available at ScienceDirect

Atmospheric Environment

journal homepage: www.elsevier.com/locate/atmosenv

Physical characterization of aerosol particles during the Chinese New Year's firework events

Min Zhang^a, Xuemei Wang^a, Jianmin Chen^{a,*}, Tiantao Cheng^a, Tao Wang^b, Xin Yang^{a,*}, Youguo Gong^c, Fuhai Geng^d, Changhong Chen^e

^a Center for Atmospheric Chemistry, Department of Environmental Science and Engineering, Fudan University, Shanghai 200433, China

^b Department of Civil and Structural Engineering, The Hong Kong Polytechnic University, Hong Kong, China

^c College of Environmental Sciences and Engineering, Peking University, Beijing 100871, China

^d Shanghai Meteorological Bureau, Shanghai 200135, China

^e Shanghai Academy of Environmental Sciences, Shanghai 200233, China

ARTICLE INFO

Article history:

Received 15 May 2010

Received in revised form

25 August 2010

Accepted 26 August 2010

Keywords:

Fireworks

Number concentration

Size distribution

Coagulation sink

Particle density

Shanghai

ABSTRACT

Measurements for particles 10 nm to 10 μm were taken using a Wide-range Particle Spectrometer during the Chinese New Year (CNY) celebrations in 2009 in Shanghai, China. These celebrations provided an opportunity to study the number concentration and size distribution of particles in an especial atmospheric pollution situation due to firework displays. The firework activities had a clear contribution to the number concentration of small accumulation mode particles (100–500 nm) and PM₁ mass concentration, with a maximum total number concentration of $3.8 \times 10^4 \text{ cm}^{-3}$. A clear shift of particles from nucleation and Aitken mode to small accumulation mode was observed at the peak of the CNY firework event, which can be explained by reduced atmospheric lifetimes of smaller particles via the concept of the coagulation sink. High particle density (2.7 g cm^{-3}) was identified as being particularly characteristic of the firework aerosols. Recalculated fine particles PM₁ exhibited on average above $150 \mu\text{g m}^{-3}$ for more than 12 hours, which was a health risk to susceptible individuals. Integral physical parameters of firework aerosols were calculated for understanding their physical properties and further model simulation.

© 2010 Elsevier Ltd. All rights reserved.

1. Introduction

Over recent years there has been increased focus on short-term air quality degradation events (Schwartz, 1996; Katsouyanni et al., 1997; Tertre et al., 2002) and their long-term negative effects to human health (Pope et al., 2002; Yorifuji et al., 2010). One of the most unusual anthropogenic activities that create notable short-term air pollution and serious health hazards is the recreational use of fireworks to celebrate festivals all over the world. In China, for example, the most intensive firework event occurs in the Chinese New Year (CNY, Spring Festival), which is the nationwide celebration every year during January or February according to lunisolar Chinese calendar with high-profile firework events occurring at midnight on the CNY's Eve in most cities and rural areas.

Burning of fireworks release gaseous pollutants such as ozone, sulfur dioxide, nitrogen oxides (Attri et al., 2001; Ravindra et al., 2003)

and suspended particles (Vecchi et al., 2008) with trace metals and organic compounds (Steinhauser et al., 2008; Moreno et al., 2007; Wang et al., 2007; Drewnick et al., 2006; Kulshrestha et al., 2004; Ravindra et al., 2003; Carranza et al., 2001; Fleischer et al., 1999; Liu et al., 1997). The short-term air quality degradation caused by fireworks often results in serious health hazards, accidents, lethal injuries (Mandal et al., 1997; Perry, 1999; Van Kamp et al., 2006; Ravindra et al., 2001; Singh et al., 2005; Witsaman et al., 2006) and a reduction in visibility for hours (Clark, 1997; Vecchi et al., 2008).

Despite the harmful effects of fireworks on air quality and human health, there is a limited amount of literatures describing the physical characteristics of firework particles. These include particle size distribution measurements from 3 to 800 nm during the Millennium fireworks in Leipzig (Wehner et al., 2000), and particle number concentrations for size $0.5 \mu\text{m} < d_p < 1 \mu\text{m}$ which increased significantly during a firework episode in Milan, Italy (up to 6.7 times within 1 h) (Vecchi et al., 2008). Measurements of particle number size distributions, in the size range of 3 to 800 nm, taken by Mönkkönen et al. (2004) during the Diwali festival in New Delhi in 2002 showed that accumulation mode particles comprised practically 100% of total particle number. A significant shift from

* Corresponding authors. Tel.: +86 21 65642298; fax: +86 21 65642080.

E-mail addresses: jmchen@fudan.edu.cn (J. Chen), yangxin@fudan.edu.cn (X. Yang).

nucleation and small Aitken mode to larger Aitken and accumulation mode particles was observed during the 2006 bonfire night celebrations in Leeds, UK (Agus et al., 2008) and 2002 Diwali festivities in New Delhi (Mönkkönen et al., 2004). The reduction and disappearance of nucleation and small Aitken mode particles can be explained via the concept of the coagulation sink, which determined how rapidly nm-size aerosol particles were removed through coagulation (Mönkkönen et al., 2004; Agus et al., 2008; Kulmala et al., 2001). Among all of physical characteristics, particle density is a parameter that directly controls particle deposition in the lungs by inertial and sedimentation processes, which may play a prominent role in consideration of the association between health effects and particulate air pollutants (Pitz et al., 2003). However, there are very few studies describing the density of firework particles. Wehner et al. (2000) calculated total sub-micrometer mass from volume size distribution by assuming a particle density of 1.7 g cm^{-3} . Collectively, most of the above measurements were either far from the centers of activities, resulting in a measurement of the advected smoke cloud, or a combination of pollution from bonfires, fireworks and traffic. Measurements of particle number size distributions associated with the CNY's fireworks in this work therefore provided a unique opportunity to study the physical characteristics of firework particles with high time resolution. The emission was large and occurred at a well-defined point in time in the absence of photochemistry, and with a minimal traffic-related contribution.

The objective of this study is to monitor the short-term variation in particle number concentrations, size distributions, modal characteristics and particle densities in the size range 10 nm to 10 μm during the 2009 firework celebrations in Shanghai, China. These measurements are compared to measurements taken prior to and following firework events. Coagulation sinks are calculated to explain the differences in particle modal patterns between the different measurement periods. In addition, particle density and integral physical parameters are calculated during the firework period. These results will serve to understand the physical characteristics of firework particles and explain the importance of the different physical processes in determining the modal characteristics.

2. Methodology

2.1. Measurement site

Measurements of concentrations and size distributions were performed continuously on the rooftop of a building on the campus of Fudan University at urban Shanghai ($31^{\circ}18'N$, $121^{\circ}29'E$) since August 2008. The site was approximately 20 m above the ground level, at a horizontal distance of approximately 200 m from one of major firework display areas. However, it should be noted that a large amount of firework displays, crackers and sparkles were set off privately in whole city throughout the National holiday (25–31 January, 2009), with the main spectacular episode started since soon after the dinner (around 18:00 LT) during the CNY's Eve (25 January, 2009), ended with the high point after midnight (0:00–1:00 LT) on 26 January, 2009. Buildings surrounding the sampling site mostly consist of commercial properties and residential dwellings, and buildings belonging to Fudan University. Collectively, factories were closed and families stayed together at home on 25 January, 2009. Fireworks were setting off after dinner on the CNY's Eve till midnight to end the day.

2.2. Instrumentation

A Wide-range Particle Spectrometer (WPSTM-model 1000 XP, MSP Corporation, USA) was used to measure aerosol size distributions in

the range of 10 nm–10 μm . The instrument is a high-resolution aerosol spectrometer which combines the principles of Differential Mobility Analysis (DMA), Condensation Particle Counting (CPC) and Laser Light Scattering (LPS) (Details can be seen in Gao et al., 2009). Before and after the field campaigns, DMA was calibrated with NIST SRM 1691 and SRM 1963 PSL spheres (0.269 μm and 0.1007 μm mean diameter) to verify proper DMA transfer function and accurate particle sizing traceable to NIST. LPS was calculated with four NIST traceable sizes of PSL (0.701 μm , 1.36 μm , 1.6 μm , and 4.0 μm mean diameter). The DMA and CPC can measure the aerosol size distributions in the 10–500 nm range in up to 96 channels. The LPS covers the 350–10,000 nm range in 24 additional channels. In the present study we chose the sample mode with 60 channels in DMA and 24 channels in LPS. Thus it took about 3 min for one complete scanning of the entire size range with 2 s of scanning period for each channel.

Ozone was measured using a Model 49i Ozone Analyzer (Thermo Fisher Scientific, Co., Ltd), together with an UV photometer which accurately and reliably measures ozone concentration in ambient air. While NO-NO₂-NO_x was measured using a Model 42i NO-NO₂-NO_x analyzer with the NO₂ to NO converter using the chemiluminescent reactions. These instruments were automatically set to zero and external calibration sources, which also met the technical specifications for US EPA (Environmental Protection Agency, <http://www.epa.gov/ttn/amtic/criteria.html>). Quality control checks were performed every day including zero, precision and span checks. Filters were replaced every two weeks, and calibration was made every three months. Ozone and NO_x were recorded each minute.

2.3. Meteorological data

Meteorological parameters such as temperature, relative humidity (RH), wind, visibility, and pressure during the observation period were provided by Shanghai Baoshan Meteorological Bureau. Daily averaged PM₁₀ used for the particle density calculation in Section 3.4 was collected from Shanghai Environmental Monitoring Center in Yangpu District (<http://www.semc.gov.cn/>), which is about 20 m above the ground level and 4 km away from our observation site. As fireworks and firecrackers were set off all over the city, it can be assumed that both our measurement site and Shanghai Environmental Monitoring Center in Yangpu District were under the similar situation.

3. Results and discussion

3.1. Number concentration and size distribution

Particles in the size range 10 nm–10 μm measured in this work are divided into 7 sub size ranges: 10–20 nm (nuclei mode), 20–50 nm and 50–100 nm (Aitken mode), 100–200 nm, 200–500 nm and 0.5–1 μm (accumulation mode), and 1–10 μm (coarse mode).

Hourly mean particle number concentrations of different size bins from 23 to 27 January 2009 are shown in Fig. 1. The figure shows that, prior to the fireworks, particle number concentrations were relatively low with two peak values around 9:00 and 18:00 rush hours, followed by a minimum during midnight around 3:00. During the main spectacular episode, which started soon after the dinner (around 18:00 LT) on 25 January and ended with the high point after midnight (0:00–1:00 LT) on 26 January, a large increase can be seen in the number concentration, with a hourly average maximum of $2.8 \times 10^4 \text{ cm}^{-3}$ during the peak hour (0:00–1:00 LT on 26 January). This concentration is almost 3 times higher than average number concentrations measured the day before at midnight. Besides, the diurnal behavior of the NO concentration is actually an indicator of the traffic density and high-temperature combustion. Less traffic can be observed on 25 January for the reason factories were mostly closed and families traditionally

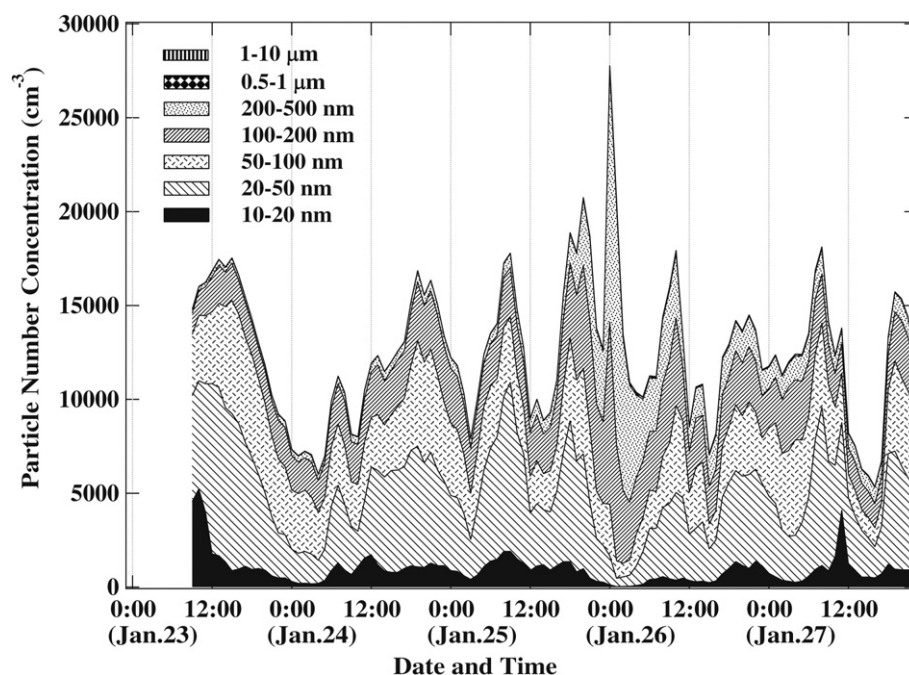


Fig. 1. Hourly mean particle number concentrations of different size bins from 23 to 27 January, 2009.

stayed together at home. A clear maximum of NO shown in Fig. 2 occurred on the CNY's Eve between 22:00 and 00:00, which correlated well with firework activities and high particle number concentrations. Whereas O₃ concentrations did not show the build-up phenomenon as Attri et al. (2001) mentioned.

Of special interest, a clear dominance and high concentrations of small accumulation mode particles (100–500 nm) were detected from 18:00 on the CNY's Eve to the day after as the main pollution source shifted to firework activities (Fig. 1). In contrast, a reduction in nucleation (96.0% and 93.9%) and Aitken mode particles (79.7% and 83.3%) was also observed during the peak hour compared to the day before and after. Nucleation and Aitken mode particles were the dominant size fractions before and after the firework event, probably due to local traffic emissions and meteorological conditions (Ferin et al., 1990). The dominance of accumulation mode particles during firework activities is in common with the results of Bonfire night (Agus et al., 2008), Diwali study (Mönkkönen et al., 2004), and recent studies of particles size distribution resulting from biomass burning during the dry season in the Amazon basin (Rissler et al., 2005).

The number size distribution during the CNY's period is shown in Fig. 3a as a contour plot. The most interesting feature of this plot is the high number concentrations of particles in the range of 100–500 nm, which dominated during the peak hour (00:00–01:00 LT on January 26) of the firework celebration, with peak value higher than $7.1 \times 10^4 \text{ cm}^{-3}$, almost twice as in normal days.

The surface area contour plot for the same time period is shown in Fig. 3b. This was calculated from the number size distribution with the assumption of spherical particles (Gao et al., 2009). This figure shows that the measured surface area distribution is dominated by particles within the accumulation mode region during the firework event, which is in common with the measurements made by Mönkkönen et al. (2004) and Wehner et al. (2000).

3.2. Coagulation sink (CoagS)

The discussion above showed that emissions from firework activities substantially changed particle size distributions as well as

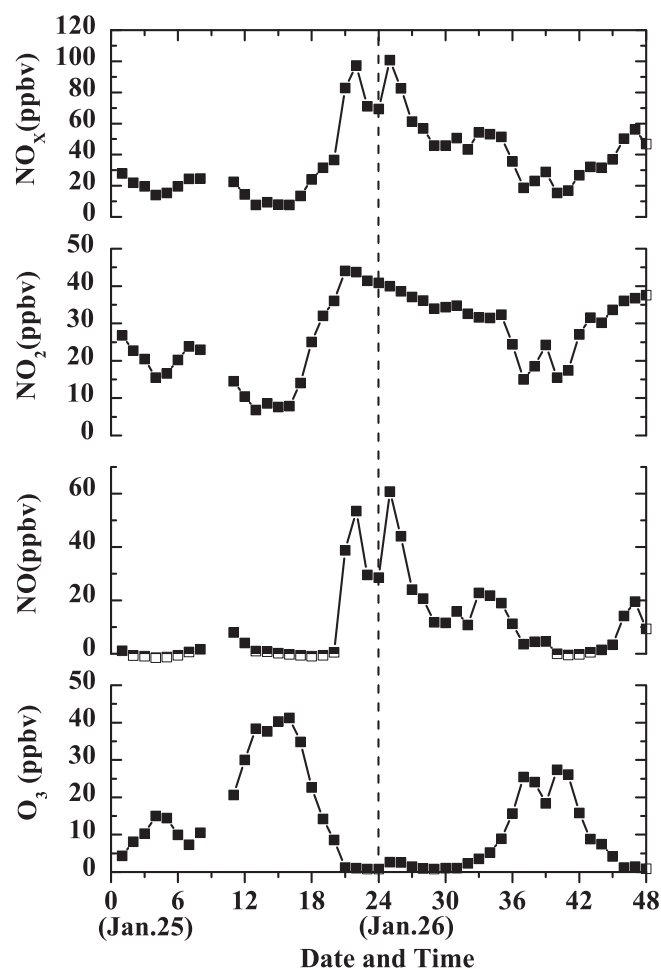


Fig. 2. Daily variation of hourly averaged O₃, NO, NO₂ and NO_x on 25 January and 26 January, 2009.

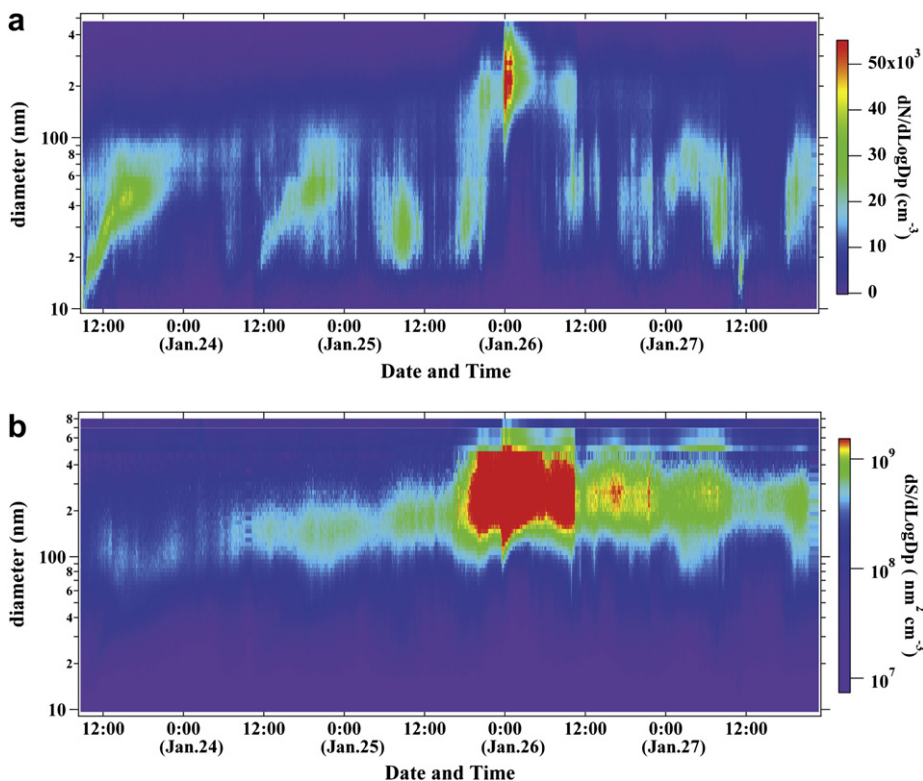


Fig. 3. Contour plots of (a) number size distribution and (b) surface area size distribution from 23 to 27 January, 2009.

increasing overall particle number concentrations. The large increase in small accumulation mode particles would be due to primary emissions from the firework celebration. Meanwhile, a reduction and disappearance of nucleation and Aitken mode particles was also observed during the firework night compared with the night before, which can be explained via the concept of the coagulation sink (Kulmala et al., 2001; Mönkkönen et al., 2004; Agus et al., 2008).

The time resolution for aerosol number concentration N in size class i can be presented by (Kulmala et al., 2001):

$$\frac{dN_i}{dt} = J_i - \text{CoagS} \times N_i \quad (1)$$

where J_i is the formation rate of particles, and the coagulation sink CoagS can be determined as:

$$\text{CoagS} = \sum_j K_{ij} N_j \quad (2)$$

where K_{ij} is coagulation coefficient between particles d_{pi} and d_{pj} ($\text{cm}^{-3} \text{s}^{-1}$, $j \geq i$), N_j is number concentration of particles size j (cm^{-3}) (Kulmala et al., 2001; Seinfeld and Pandis, 1998).

Equation (2) has the following “pseudo steady-state solution”

$$N_i = \frac{J_i}{\text{CoagS}} \quad (3)$$

Thus, a large coagulation sink value implies a small concentration of nucleation or Aitken mode particles (and vice versa), assuming a constant source J_i (Mönkkönen et al., 2004).

Coagulation sink values were calculated for the particle diameters of 1, 5, 10, 20, 50, 100 nm throughout the firework activities (Fig. 4). These sinks are based on coagulation to particles $\leq 10 \mu\text{m}$, the upper limit of the WPS used in this experiment. The coagulation sink values during the firework celebration were overall very high in comparison to the other periods studied. The maximum

Table 1
Modeled coagulation sinks and characteristics lifetime of 1 nm and 100 nm particles compared with those in Mönkkönen et al. (2004) and Agus et al. (2008).

Parameter	This study	Agus et al., 2008	Mönkkönen et al., 2004
	Fireworks	Bonfire and fireworks	Fireworks
<i>1 nm</i>			
CoagS (s^{-1})	0.146	0.0371	0.673
Lifetime (s)	6.85	27.0	1.49
Lifetime (h)	0.0019	0.0075	4.13×10^{-4}
<i>100 nm</i>			
CoagS (s^{-1})	6.98×10^{-5}	1.94×10^{-5}	2.04×10^{-4}
Lifetime (s)	14326.65	51666.12	4901.96
Lifetime (h)	3.98	14.35	1.36

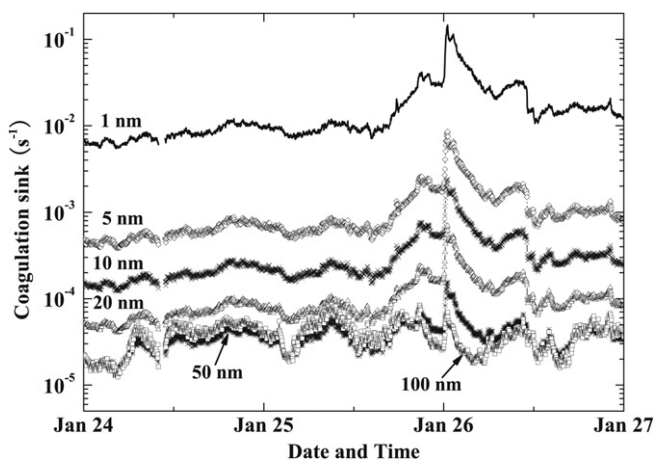


Fig. 4. Coagulation sinks for different particle sizes during the CNY Period.

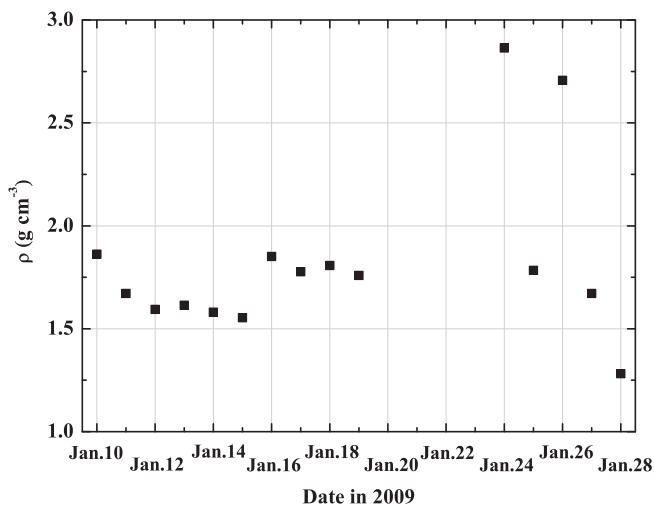


Fig. 5. Scatter plot of daily averaged apparent particle density ρ in January, 2009.

coagulation sink values for 1 and 100 nm particles were 0.146 s^{-1} and $6.98 \times 10^{-5} \text{ s}^{-1}$ at the same time, respectively. Another way of looking at this issue is the inverse of the coagulation sink, which can be considered to be representative of the characteristic lifetime of particles. Thus, calculated lifetimes of 1 and 100 nm particles were roughly seconds and hours during the firework event, respectively. Therefore, it was natural that high concentrations of nucleation and Aitken mode particles could not be detected during the firework event.

Coagulation sinks estimated in this study are compared with those from Agus et al. (2008) and Mönkkönen et al. (2004) shown in Table 1. Our results are intermediate between the two other studies. Three reasons for the differences can be suggested. Firstly, the total particle number concentrations in the Mönkkönen et al. (2004) study were about a factor of three higher than those detected in our study and Agus et al. (2008), which probably indicated that higher number concentrations led to higher coagulation sinks. Secondly, measurements taken by Agus et al. (2008) only showed the results from 4.7 to 160 nm indicated that they had a relatively lower contribution to overall coagulation sinks. The dominant size fraction for firework particles was proved to be in the range of 100–500 nm in this study. Thus missing data of larger size particles by Agus et al. (2008) led to relatively lower coagulation sinks. Thirdly, results in our work and Mönkkönen et al. (2004) were more reflected firework particles, while Agus et al. (2008) study was affected by a mixed pollution event of bonfire and fireworks with smaller detected size range (4.7–160 nm). However, it is hard to estimate separately the contribution of bonfire particles to coagulation sinks.

3.3. Particle density

One of the main problems encountered in this work is to relate ambient particle number to mass, which needs to make assumptions about the particle density. The particle density was calculated in this work by the following equation (Pitz et al., 2003):

$$\rho = \frac{M_{PM_{10}}}{V_W} \quad (4)$$

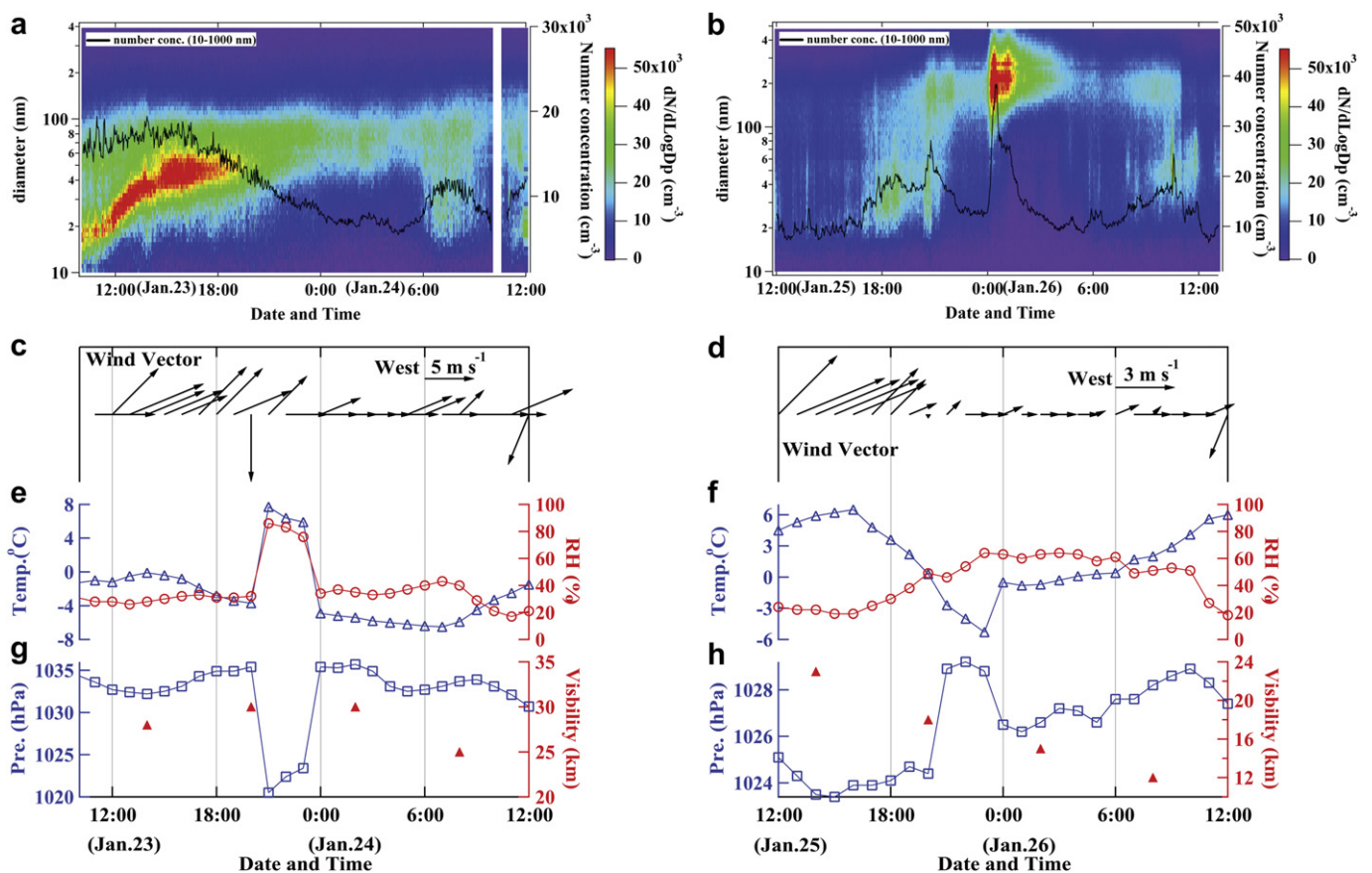


Fig. 6. Daily variation of number size distributions and number concentrations (a, b) as well as corresponding meteorological parameters (c–h) during 23–24 January and 25–26 January, 2009.

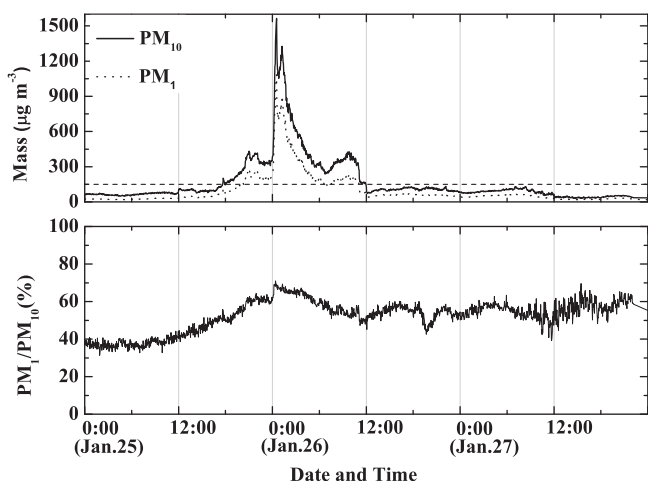


Fig. 7. Time series of recalculated PM₁₀, PM₁ and PM₁ to PM₁₀ ratio, with the dotted line stands for National Ambient Air Quality Standards of PM₁₀ (24 h, 150 µg m⁻³).

where $M_{PM_{10}}$ (µg m⁻³) is the daily averaged PM₁₀ mass concentration in the sampling district which was reported from Shanghai Environmental Monitoring Center (<http://www.semc.gov.cn/>). $M_{PM_{10}}$ on 26 January stands for the period from 12:00 LT on 25 January to 12:00 LT on 26 January, 2009. V_W (µm⁻³ cm⁻³) is calculated by integrating the volume size distribution from 10 nm up to an aerodynamic diameter of 10 µm, assuming an apparent density 1 g cm⁻³ and particles to be spherical shaped. Thus apparent density ρ (g cm⁻³) is the daily averaged particle density, calculated as the ratio of particle mass concentration on a daily basis to the corresponding volume concentration.

Daily averaged particle density ρ in January is shown in Fig. 5. The loss of data during 20–23 January was due to rainy days. The daily arithmetic mean density of particles up to 10 µm was generally between 1.5 and 2.0 g cm⁻³, with the exception of two significantly

higher values of 2.9 and 2.7 g cm⁻³ which occurred on 24 January and 26 January respectively. The results calculated here are quite near to previous studies. Hänel and Thudium (1977) determined particle density up to 3.0 g cm⁻³ with the range of 1.8–3.0 g cm⁻³ at Mainz, BRD for dry atmospheric aerosol, mean value 1.6 ± 0.5 g cm⁻³ with the range 1.0–2.5 g cm⁻³ for urban aerosol in Erfurt, Germany (Pitz et al., 2003). In addition, 1.0–1.5 g cm⁻³ for ambient aerosol was reported in Riverside, California (Spencer et al., 2007); 1.2–1.8 g cm⁻³ in Summer during high humidity period in Queensland, Australia (Morawska et al., 1999); 1.3–2.0 g cm⁻³ for ambient aerosols during summer season 1999 on GSF campus, Germany (Karg, 2000); and 1.6–1.8 g cm⁻³ for ambient aerosols Meadview, AZ, and Minneapolis, MN, USA (Stein et al., 1994).

The large scale of particle density indicated different factors and emission sources affecting the particle formation. The two high particle density periods occurred on 24 January and 26 January were chosen here for comparison. Fig. 6 shows the daily variation of number size distributions and number concentrations as well as corresponding meteorological parameters of two periods. Different from “banana events” for indicating new particle formation, nucleation and growth process (Gao et al., 2009; Heintzenberg et al., 2007; Kulmala et al., 2000), the “tadpole event” on 23–24 January (Fig. 6a) began at 10 nm was more possibly indicating secondary aerosol formation and growth process. Higher wind speed (Fig. 6c) with extremely low RH (Fig. 6e) indicates the other possible reason for higher particle density by bringing road dust and western industrial sources in a much dryer environment, as indicated by Hänel and Thudium (1977).

Compared with that on 23–24 January, the firework celebration on 25–26 January (Fig. 6b) was an unusual source for new particle production with much higher number concentration of 3.8×10^4 cm⁻³ (Fig. 6b) in short time period. Due to stable weather conditions (low wind speed (0–2 m s⁻¹), weak variations in RH, temperature and pressure, Fig. 6d, f, h), dispersal of the enhanced levels of aerosol particles generated by fireworks was inhibited and particles were “trapped and accumulated” within an ageing air

Table 2
Integral physical properties calculated from particle size distributions during the peak hour (0:00–1:00 LT on 26 January, 2009). $D_{low} = 10$ nm, $D_{high} = 10$ µm, $D_1 = 500$ nm, $D_2 = 100$ nm.

No.	ID	Parameter	Calculated value	Unit	Definition
1	N_T	Total number	27,705 ± 6850	cm ⁻³	α
2	L_T	Total length	5895 ± 1738	µm cm ⁻³	β
3	S_T	Total surface	5228 ± 1636	µm ² cm ⁻³	γ
4	V_T	Total volume	389 ± 119	µm ³ cm ⁻³	δ
5	M_T	Total mass (PM ₁₀)	1054 ± 322	µg m ⁻³	ρV ($\rho = 2.71$ g cm ⁻³ see section 3.3)
6	N_1	Number ≤ D_1	27,487 ± 6801	cm ⁻³	As in parameter 1 but for $D_{high} = D_1$
7	L_1	Length ≤ D_1	5726 ± 1696	µm cm ⁻³	As in parameter 2 but for $D_{high} = D_1$
8	S_1	Surface ≤ D_1	4685 ± 1495	µm ² cm ⁻³	As in parameter 3 but for $D_{high} = D_1$
9	V_1	Volume ≤ D_1	239 ± 79	µm ³ cm ⁻³	As in parameter 4 but for $D_{high} = D_1$
10	M_1	Mass ≤ D_1 (PM _{0.5})	648 ± 214	µg m ⁻³	ρV ($\rho = 2.71$ g cm ⁻³ see section 3.3)
11	N_2	Number ≤ D_2	4813 ± 1001	cm ⁻³	As in parameter 1 but for $D_{high} = D_2$
12	L_2	Length ≤ D_2	308 ± 66	µm cm ⁻³	As in parameter 2 but for $D_{high} = D_2$
13	S_2	Surface ≤ D_2	71 ± 16	µm ² cm ⁻³	As in parameter 3 but for $D_{high} = D_2$
14	V_2	Volume ≤ D_2	0.93 ± 0.23	µm ³ cm ⁻³	As in parameter 4 but for $D_{high} = D_2$
15	M_2	Mass ≤ D_2	2.52 ± 0.62	µg m ⁻³	$\rho_2 V$ ($\rho = 2.71$ g cm ⁻³ see section 3.3)
16	\bar{D}_N	Mean Number diameter ≤ D_1	196 ± 18	nm	ϵ
17	\bar{D}_L	Mean length diameter ≤ D_1	248 ± 12	nm	ζ
18	\bar{D}_S	Mean surface diameter ≤ D_1	289 ± 9	nm	η
19	\bar{D}_V	Mean volume diameter ≤ D_1	320 ± 6	nm	θ
20	D_N	Median Number diameter ≤ D_1	180 ± 6	nm	ι
21	D_L	Median length diameter ≤ D_1	231 ± 7	nm	κ
22	D_S	Median surface diameter ≤ D_1	277 ± 10	nm	ν
23	D_V	Median volume diameter ≤ D_1	313 ± 12	nm	ξ

$$\alpha: \int_{\log D_{low}}^{\log D_{high}} \frac{dn(\log D_p)}{d\log D_p} d\log D_p, \quad \beta: \int_{\log D_{low}}^{\log D_{high}} \frac{dn(\log D_p)}{d\log D_p} D_p d\log D_p, \quad \gamma: 4\pi \int_{\log D_{low}}^{\log D_{high}} \frac{dn(\log D_p)}{d\log D_p} \left(\frac{D_p}{2}\right)^2 d\log D_p, \quad \delta: \frac{4}{3}\pi \int_{\log D_{low}}^{\log D_{high}} \frac{dn(\log D_p)}{d\log D_p} \left(\frac{D_p}{2}\right)^3 d\log D_p, \quad \epsilon: \int_{\log D_{low}}^{\log D_1} \frac{dn(\log D_p)}{d\log D_p} D_p d\log D_p / N_1,$$

$$\zeta: \int_{\log D_{low}}^{\log D_1} \frac{dn(\log D_p)}{d\log D_p} D_p d\log D_p / L_1, \quad \eta: 4\pi \int_{\log D_{low}}^{\log D_1} \frac{dn(\log D_p)}{d\log D_p} \left(\frac{D_p}{2}\right)^2 D_p d\log D_p / S_1, \quad \theta: \frac{4}{3}\pi \int_{\log D_{low}}^{\log D_1} \frac{dn(\log D_p)}{d\log D_p} \left(\frac{D_p}{2}\right)^3 D_p d\log D_p / V_1, \quad \iota: \int_{\log D_{low}}^{\log D_N} \frac{dn(\log D_p)}{d\log D_p} d\log D_p = \frac{1}{2}N_1,$$

$$\kappa: \int_{\log D_{low}}^{\log D_1} \frac{dn(\log D_p)}{d\log D_p} D_p d\log D_p = \frac{1}{2}L_1, \quad \nu: 4\pi \int_{\log D_{low}}^{\log D_1} \frac{dn(\log D_p)}{d\log D_p} \left(\frac{D_p}{2}\right)^2 d\log D_p = \frac{1}{2}S_1, \quad \xi: \frac{4}{3}\pi \int_{\log D_{low}}^{\log D_1} \frac{dn(\log D_p)}{d\log D_p} \left(\frac{D_p}{2}\right)^3 d\log D_p = \frac{1}{2}V_1.$$

mass. Combined with large amounts of metallic and organic composition generated by fireworks (Wang et al., 2007), the particle density was much higher than normal days.

In sum, the two high particle density episodes here possibly stood for two extremes: (1) 23–24 January was possibly strongly influenced by secondary particle production process, dry environment and possibly local sources; (2) 25–26 January was strongly influenced by large amount of firework emissions and then accumulation processes caused by stable weather condition.

Additionally, based on the density data shown in Fig. 5, time series of recalculated PM₁₀, PM₁ and PM₁ to PM₁₀ ratios from the number size distribution 10 nm–10 μm are shown in Fig. 7, with the dotted line stands for National Ambient Air Quality Standards of PM₁₀ (24 h, 150 μg m⁻³). Fine particles (PM₁) accounted for more than 40% of PM₁₀, rising to more than 60% during the period of firework displays. It can be seen that the concentration of PM₁₀ was much more than 150 μg m⁻³ from 18:00 LT on 25 January to 12:00 LT on 26 January. The following two days were still in high PM₁₀ concentration close to 150 μg m⁻³, with the PM₁ to PM₁₀ ratios fluctuating around 50%.

3.4. Integral physical parameters

A number of integral physical parameters were calculated based on particle number size distributions and particle density during the peak hour (00:00–01:00 LT on 26 January), which were explored for understanding the physical properties of firework particles. By calculating these integral parameters not only for the total size range from 10 nm to 10 μm but also in two sub-ranges, a total of 23 parameters were derived, which are listed in Table 2.

As particles between 100 and 500 nm were the dominant size fraction during the firework period, D_1 was defined to be 500 nm and D_2 as 100 nm. The calculated results in Table 2 showed that PM₁₀ could be as high as $1054 \pm 322 \mu\text{g m}^{-3}$ during the peak hour, with the mean particle sizes were 196 ± 18 (number), 248 ± 12 (length), 289 ± 9 (surface) and 320 ± 6 nm (volume), respectively. Besides, the median particle sizes were 180 ± 6 (number), 231 ± 7 (length), 277 ± 10 (surface) and 313 ± 12 nm (volume), respectively. The size range from 100 to 500 nm contributed to about 82%, 92%, 88% and 61% to the total number, length, surface and volume (mass) concentrations, respectively. The results demonstrate that firework activities had a clear contribution to aerosol number size distributions and PM₁₀ mass concentrations. Primary emissions of firework particles are in the smaller accumulation mode region, which significantly alter the modal structure of particle size distributions.

As for the statistics in Table 2 was only the main burning period, the variation of the whole firework burning period needs more studies and discussion. However, these parameters would be helpful for understanding the physical properties of fireworks aerosol and further model simulation.

4. Conclusion

Aerosol particle number concentrations and size distributions in the diameter range of 10 nm to 10 μm were measured during the CNY's firework event in 2009 in Shanghai, China. Particle concentrations during the peak hour of firework celebrations were approximately 3 times higher than the day before, with a clear shift of particles from nucleation and Aitken mode to small accumulation mode. Coagulation sinks for all particle sizes were greatly enhanced during the firework celebration due to high concentrations of accumulation mode particles. The maximum coagulation sink values for 1 and 100 nm particles were 0.146 s^{-1} and $6.98 \times 10^{-5} \text{ s}^{-1}$ during the peak hour, respectively. Thus, lifetimes of 1 and 100 nm particles were in the order of seconds and hours,

respectively, resulting in reduction and disappearance of smaller particles.

Daily averaged particle density was calculated as high as 2.7 g cm^{-3} , which would be one of the parameters that directly control particle deposition in lungs by inertial and sedimentation processes. A number of integral physical parameters were also concluded for understanding the physical properties of particles generated from firework displays.

The results demonstrate that primary emissions from firework celebrations significantly alter the modal structure of particle size distributions and particle density. Both these properties are likely to influence particle radiative properties and toxicological effects.

Acknowledgements

We would like to thank Dr. Jian Gao in Chinese Research Academy of Environmental Sciences, Ms. Dingli Yue in Peking University for their helpful suggestions for calculation process. This research was supported by the National Natural Science Foundation of China (Nos. 40875073, 40722006, 40775079, 20937001), Shanghai Dawn Program (08SG07), Hundred Talents Program of the Chinese Academy of Sciences, Science & Technology Commission of Shanghai Municipality (No.09160707700) and Key Project (No. 108050) from Ministry of Education of China. Data analysis work was partially supported by The Hong Kong Polytechnic University's Mainland Joint Supervision Scheme (Project No. GU-635).

References

- Agus, E.L., Lingard, J.J.N., Tomlin, A.S., 2008. Suppression of nucleation mode particles by biomass burning in an urban environment: a case study. *Journal of Environmental Monitoring* 10, 979–988.
- Attri, A.K., Kumar, U., Jain, V.K., 2001. Microclimate – formation of ozone by fireworks. *Nature* 411 (6841), 1015.
- Carranza, J.E., Fisher, B.T., Yoder, G.D., Hahn, D.W., 2001. On-line analysis of ambient air aerosols using laser-induced breakdown spectroscopy. *Spectrochimica Acta, Part B Atomic Spectroscopy* 56 (6), 851–864.
- Clark, H., 1997. New directions – light blue touch paper and retire. *Atmospheric Environment* 31 (17), 2893–2894.
- Drewnick, F., Hings, S.S., Curtius, J., Eerdeken, G., Williams, J., 2006. Measurement of fine particulate and gas-phase species during the New Year's fireworks 2005 in Mainz, Germany. *Atmospheric Environment* 40 (23), 4316–4327.
- Ferin, J., Oberdoerster, G., Penney, D.P., Soderholm, S.C., Gelein, R., Piper, H.C., 1990. Increased pulmonary toxicity of ultrafine particles I. Particle clearance, translocation, morphology. *Journal of Aerosol Science* 21 (3), 381–384.
- Fleischer, O., Wichmann, H., Lorenz, W., 1999. Release of polychlorinated dibenzo-p-dioxins and dibenzofurans by setting off fireworks. *Chemosphere* 39 (6), 925–932.
- Gao, J., Wang, T., Zhou, X.H., Wu, W.S., Wang, W.X., 2009. Measurement of aerosol number size distributions in the Yangtze River delta in China: formation and growth of particles under polluted conditions. *Atmospheric Environment* 43 (4), 829–836.
- Hänel, G., Thudium, J., 1977. Mean bulk densities of samples of dry atmospheric aerosol-particles – summary of measured data. *Pure and Applied Geophysics* 115 (4), 799–803.
- Heintzenberg, J., Wehner, B., Birmili, W., 2007. 'How to find bananas in the atmospheric aerosol': new approach for analyzing atmospheric nucleation and growth events. *Tellus* 59B, 273–282.
- Karg, E., 2000. Density of ambient particles from combined DMA and APS data. *Journal of Aerosol Science* 31, 759–760.
- Katsouyanni, K., Touloumi, G., Spix, C., Schwartz, J., Balducci, F., Medina, S., Rossi, G., Wojtyniak, B., Sunyer, J., Bacharova, L., Schouten, J.P., Ponka, A., Anderson, H.R., 1997. Short term effects of ambient sulphur dioxide and particulate matter on mortality in 12 European cities: results from time series data from the APHEA project. *Air pollution and health: an European approach*. *British Medical Journal* 314, 1658–1663.
- Kulmala, M., Pirjola, U., Mäkelä, J.M., 2000. Stable sulphate clusters as a source of new atmospheric particles. *Nature* 404 (6773), 66–69.
- Kulmala, M., Dal Maso, M., Mäkelä, J.M., Pirjola, L., Väkevä, M., Aalto, P., Miikkulainen, P., Hämeri, K., O'Dowd, C.D., 2001. On the formation, growth and composition of nucleation mode particles. *Tellus* 53B, 479–490.
- Kulshrestha, U.C., Nageswara Rao, T., Azhagavel, S., Kulshrestha, M.J., 2004. Emissions and accumulation of metals in the atmosphere due to crackers and sparkles during Diwali festival in India. *Atmospheric Environment* 38, 4421–4425.
- Liu, D.Y., Rutherford, D., Kinsey, M., Prather, K.A., 1997. Real-time monitoring of pyrotechnically derived aerosol particles in the troposphere. *Analytical Chemistry* 69 (10), 1808–1814.

- Mandal, R., Sen, B.K., Sen, S., 1997. Impact of fireworks on our environment. *Indian Journal of Environmental Protection* 17, 850–853.
- Mönkkönen, P., Koponen, I.K., Lehtinen, K.E.J., Uma, R., Srinivasan, D., Hämeri, K., Kulmala, M., 2004. Death of nucleation and Aitken mode particles: observations at extreme atmospheric conditions and their theoretical explanation. *Journal of Aerosol Science* 35, 781–787.
- Morawska, L., Johnson, G.R., Ristovski, Z., Agranovski, V., 1999. Relation between particle mass and number for submicrometer airborne particles. *Atmospheric Environment* 33 (13), 1983–1990.
- Moreno, T., Querol, X., Alastuey, A., Minguillon, M.C., Pey, J., Rodriguez, S., Miro, J.V., Felis, C., Gibbons, W., 2007. Recreational atmospheric pollution episodes: inhalable metalliferous particles from firework displays. *Atmospheric Environment* 41 (5), 913–922.
- Perry, K.D., 1999. Effects of outdoor pyrotechnic displays on the regional air quality of Western Washington State. *Journal of the Air & Waste Management Association* 49, 146–155.
- Pitz, M., Cyrys, J., Karg, E., Wiedensohler, A., Wichmann, H.E., Heinrich, J., 2003. Variability of apparent particle density of an urban aerosol. *Environmental Science and Technology* 37 (19), 4336–4342.
- Pope, C., Burnett, R., Thun, M., Calle, E., Krewski, D., Ito, K., Thurston, G., 2002. Lung cancer, cardiopulmonary mortality, and long-term exposure to fine particulate air pollution. *Journal of the American Medical Association* 287, 1132–1141.
- Ravindra, K., Mittal, A.K., Van Grieken, R., 2001. Health risk assessment of urban suspended particulate matter with special reference to polycyclic aromatic hydrocarbons: a review. *Review on Environmental Health* 16 (3), 169–189.
- Ravindra, K., Mor, S., Kaushik, C.P., 2003. Short-term variation in air quality associated with firework events: a case study. *Journal of Environmental Monitoring* 5 (2), 260–264.
- Rissler, J., Vestin, A., Swietlicki, E., Fisch, G., Zhou, J., Artaxo, P., Andreae, M.O., 2005. Size distribution and hygroscopic properties of aerosol particles from dry-season biomass burning in Amazonia. *Atmospheric Chemistry and Physics Discussions* 5, 8149–8207.
- Schwartz, J., 1996. Air pollution and hospital admissions for respiratory disease. *Epidemiology* 7, 20–28.
- Seinfeld, J.H., Pandis, S.N., 1998. *Atmospheric Chemistry and Physics: From Air Pollution to Climate Change* (M). Wiley, New York.
- Singh, D.V., Sharma, Y.R., Azad, R.V., 2005. Visual outcome after fireworks injuries. *The Journal of Trauma* 59 (1), 109–111.
- Spencer, M.T., Shields, L.G., Prather, K.A., 2007. Simultaneous measurement of the effective density and chemical composition of ambient aerosol particles. *Environmental Science and Technology* 41 (4), 1303–1309.
- Stein, S.W., Turpin, B.J., Cai, X.P., Huang, C.P.F., McMurry, P.H., 1994. Measurements of relative humidity-dependent bounce and density for atmospheric particles using the Dma-Impactor technique. *Atmospheric Environment* 28 (10), 1739–1746.
- Steinhauser, G., Sterba, J.H., Foster, M., Grass, F., Bichler, M., 2008. Heavy metals from pyrotechnics in New Years Eve snow. *Atmospheric Environment* 42 (37), 8616–8622.
- Tertre, A., Medina, S., Samoli, E., Forsberg, B., Michelozzi, P., Boumghar, A., Vonk, J.M., Bellini, A., Atkinson, R., Ayres, J.G., Sunyer, J., Schwartz, J., Katsouyanni, K., 2002. Short-term effects of particulate air pollution on cardiovascular diseases in eight European cities. *Journal of Epidemiology and Community Health* 56, 773–779.
- Van Kamp, I., Van der Velden, P.G., Stellato, R.K., Roorda, J., Van Loon, J., Kleber, R.J., Gersons, B.B.R., Lebet, E., 2006. Physical and mental health shortly after a disaster: first results from the Enschede firework disaster study. *The European Journal of Public Health* 16 (3), 252–258.
- Vecchi, R., Bernardoni, V., Cricchio, D., D'Alessandro, A., Fermo, P., Lucarelli, F., Nava, S., Plazzalunga, A., Valli, G., 2008. The impact of fireworks on airborne particles. *Atmospheric Environment* 42 (6), 1121–1132.
- Wang, Y., Zhuang, G.S., Xu, C., An, Z.S., 2007. The air pollution caused by the burning of fireworks during the lantern festival in Beijing. *Atmospheric Environment* 41 (2), 417–431.
- Wehner, B., Wiedensohler, A., Heintzenberg, J., 2000. Submicrometer aerosol size distributions and mass concentration of the millennium fireworks 2000 in Leipzig, Germany. *Journal of Aerosol Science* 31 (12), 1489–1493.
- Witsaman, R.J., Comstock, R.D., Smith, G.A., 2006. Pediatric fireworks-related injuries in the United States: 1990–2003. *Pediatrics* 118 (1), 296–303.
- Yorifuji, T., Kashima, S., Tsuda, T., Takao, S., Suzuki, E., Doi, H., Sugiyama, M., Ishikawa-Takata, K., Ohta, T., 2010. Long-term exposure to traffic-related air pollution and mortality in Shizuoka, Japan. *Occupational and Environmental Medicine* 67, 111–117.